Binding Site Elucidation of Hydantoin-Based Antagonists of LFA-1 Using Multidisciplinary Technologies: Evidence for the Allosteric Inhibition of a Protein−Protein Interaction

Kathleen Last-Barney,[†] Walter Davidson,[†] Mario Cardozo,[†] Leah L. Frye, Christine A. Grygon, Jerry L. Hopkins, Deborah D. Jeanfavre, Susan Pav, Chungeng Qian, James M. Stevenson, Liang Tong,[‡] Renee Zindell, and Terence A. Kelly*

Contribution from the Research and Development Center, Boehringer Ingelheim Pharmaceuticals, 900 Ridgebury Road, P.O. Box 368, Ridgefield, Connecticut 06877

Received February 16, 2001

Abstract: The binding site on the lymphocyte function-associated antigen-1 (LFA-1) of a class of hydantoin-based antagonists of leukocyte cell adhesion has been identified. This site resides in the inserted-domain (I-domain) of the CD11a chain at a location that is distal to residues known to be required for interactions with the intercellular adhesion molecules. This finding supports the hypothesis that the molecules are antagonizing cell adhesion via an allosteric modification of LFA-1. The binding site was identified using an integrated immunochemical, chemical, and molecular modeling approach. Antibodies that map to epitopes on the I-domain were blocked from binding to the purified protein by the hydantoins, indicating that the hydantoin-binding site resides on the I-domain. Photoaffinity labeling of the I-domain followed by LC/MS and LC/MS/MS analysis of the enzymatic digest identified proline 281 as the primary amino acid residue covalently attached to the photoprobe. Distance constraints derived from this study coupled with known SAR considerations allowed for the construction of a molecular model of the I-domain/inhibitor complex. The atomic details of the protein/antagonist interaction were accurately predicted by this model, as subsequently confirmed by the X-ray crystal structure of the complex.

The interactions between the lymphocyte function-associated antigen-1 (LFA-1; CD11a, CD18; integrin $\alpha_L\beta_2$) and its ligands, the intercellular adhesion molecules 1−3 (ICAMs), play a critical role in leukocyte adhesion.[1−3] Individuals who lack the expression of functional CD18 have a rare leukocyte adhesion deficiency (LAD) and present clinically with recurrent infections due to their inability to mount normal inflammatory responses,[4] indicating the necessity of the β_2 integrins in immune function. In the case of overactive immune responses and inflammatory conditions, the attenuation of LFA-1-mediated cell adhesion offers potential as therapy for a number of disease states. Support for this approach comes from animal models in which antibodies directed against LFA-1 display immunosuppressive activity in vivo.[5,6] Furthermore, recent publications have reported positive results for anti-LFA-1 antibodies in early (phase II) clinical trials on transplantation[7,8] and psoriasis.[9]

Chart 1

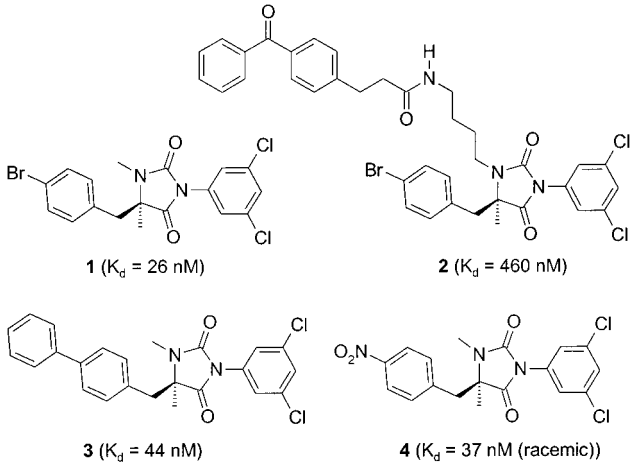

We have recently reported the discovery of BIRT377 (**1**; Chart 1),[10] a member of a novel class of low molecular weight hydantoins which are potent antagonists of LFA-1-mediated cell

* To whom correspondence should be addressed. E-mail: tkelly@rdg.boehringer-ingelheim.com.

† These individuals contributed equally to this work.

‡ Current address: Department of Biological Sciences, Columbia University, New York, NY 10027.

(1) Springer, T. A. *Nature* **1990**, *346*, 425−34.

(2) Gahmberg, C. G. *Curr. Opin. Cell Biol.* **1997**, *9*, 643−50.

(3) Vazeux, R., P.; Hoffman, A.; Tomita, J. K.; Dickinson, E. S.; Jasman, R. L.; St. John, T.; Gallatin, W. M. *Nature* **1992**, *360*, 485−8.

(4) Anderson, D. C.; Springer, T. A. *Annu. Rev. Med.* **1987**, *38*, 175−94.

(5) Kishimoto, T. K.; Rothlein, R. *Adv. Pharmacol. (New York)*, **1994**, *25*, 117−69.

(6) Gorski, A. *Immunol. Today* **1994**, *15*, 251−5.

(7) Fischer, A.; Friedrich, W.; Fasth, A.; Blanche, S.; Le Deist, F.; Girault, D.; Veber, F.; Vossen, J.; Lopez, M.; Griscelli, C. *Blood* **1991**, *77*, 249−56.

(8) Hourmant, M.; Le Mauff, B.; Le Meur, Y.; Dantal, J.; Cantarovich, D.; Giral, M.; Caudrelier, P.; Albericci, G.; Soulillou, J. P. *Transplantation* **1994**, *58*, 377−80.

(9) Gottlieb, A.; Krueger, J. G.; Bright, R.; Ling, M.; Lebwohl, M.; Kang, S.; Feldman, S.; Spellman, M.; Wittkowski, K.; Ochs, H. D.; Jardieu, P.; Bauer, R.; White, M.; Dedrick, R.; Garavoy, M. *J. Am. Acad. Dermatol.* **2000**, *42*, 428−35.

(10) Kelly, T. A.; Jeanfavre, D. D.; McNeil, D. W.; Woska, J. R., Jr.; Reilly, P. L.; Mainolfi, E. A.; Kishimoto, K. M.; Nabozny, G. H.; Zinter, R.; Bormann, B.-J.; Rothlein, R. *J. Immunol.* **1999**, *163*, 5173−7.

10.1021/ja0104249 CCC: $20.00
Published on Web 05/26/2001

Scheme 1. Synthesis of Benzophenone Photoprobe **2**

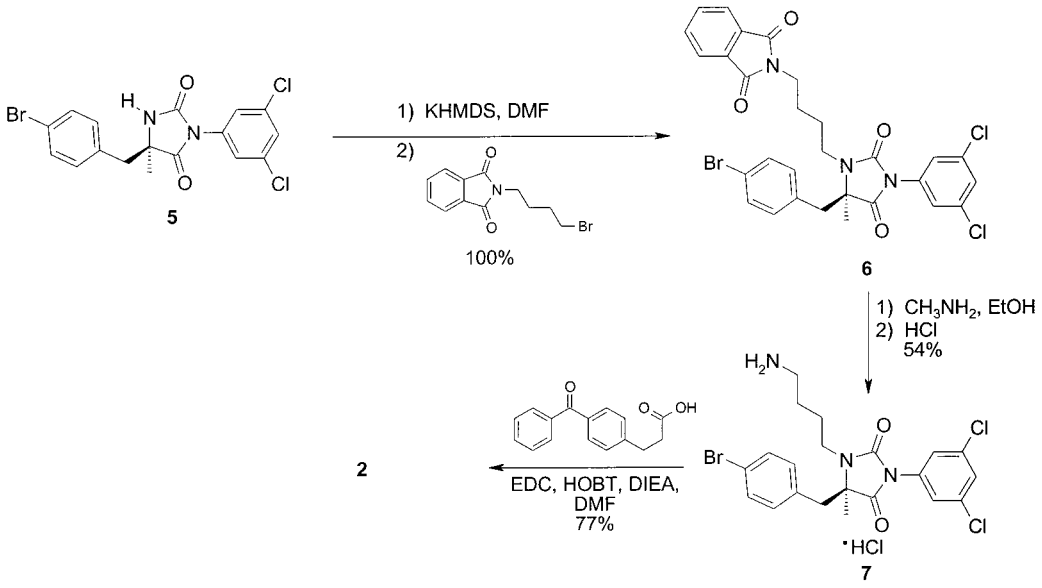

adhesion and may have potential as therapeutic agents in autoimmune diseases. The compounds are unique from other known antagonists of large protein/protein interactions[11,12] in that they are lipophilic, nonpolar molecules that do not appear to function by mimicking essential surface contact epitopes. Furthermore, the compounds block the binding of an anti-CD11a antibody that selectively recognizes an active conformation of LFA-1.[13] These observations led to the hypothesis that the compounds act via allosteric means to drive the equilibrium between active and inactive states of LFA-1 toward the conformation that does not support ICAM-1 binding. In this report, the specific binding site of this class of inhibitors on the inserted- ("I-") domain of LFA-1 has been identified through an integrated immunochemical, chemical, and molecular modeling approach. The calculated binding mode of the inhibitor agrees with high fidelity to coordinates subsequently generated using protein X-ray crystallography and supports the proposed mechanism of integrin regulation by allosteric modification of conformational equilibrium.

LFA-1 is a heterodimeric protein comprising the CD18 subunit, common to all β_2 integrins, and the CD11a subunit, unique to LFA-1.[1] The CD11a chain is proposed to have a stalklike structure upon which rests a multidomain β-propeller motif.[14] Inserted between two of the domains of the β-propeller is the ~200-amino acid I-domain.[15]

The interactions that support binding of ICAM-1 to LFA-1 encompass a large surface area.[16] Several lines of study indicate that the regions of contact primarily involve the first immunoglobulin domain of ICAM-1,[17,18] as well as portions of the β-propeller and the I-domain of CD11a.[19−24] In particular, the metal ion-dependent adhesion site (MIDAS) motifs on the β_2 integrin I-domains are involved in the coordination of divalent cations known to be essential for binding the ICAMs.[25,26]

We have previously studied the effect of BIRT377 on antibody binding to isolated LFA-1 and demonstrated that the compound binds to the CD11a chain and affects the presentation of some, but not all, epitopes that map to the I-domain.[10] Antibody R3.1 maps to an epitope on the I-domain and is blocked from binding to purified full length LFA-1 by BIRT377.[10] Subsequent experiments exploring the ability of BIRT377 to block the binding of R3.1 to recombinant CD11a I-domain confirmed that the binding site is, in fact, on the I-domain (data not shown).

Photoaffinity labeling experiments were performed to locate the amino acid residues comprising the BIRT377 binding site. The benzophenone photoprobe (**2**; Chart 1) was synthesized from known intermediates[27] as shown in Scheme 1 and has a K_d of 460 nM in the LFA-1/ICAM-1 binding assay.[10] The probe was incubated with the recombinant CD11a I-domain and the mixture irradiated with UV light to generate a stable covalent adduct of probe and protein.[28] The covalently modified protein and the untreated protein control were digested with trypsin and analyzed by μHPLC/ESI MS. For every peptide observed in the unlabeled tryptic digest, the mass of the corresponding theoretical peptide having the same sequence plus the mass (+736 amu) from the photoprobe (along with the *m*/*z* values of probable charge states) was calculated. The tryptic digest of the photolabeled sample was analyzed by the same μHPLC/

(11) Ruoslahti, E.; Pierschbacher, M. D. *Cell* **1986**, *44*, 517.
(12) Zimmerman, C. N. *Exp. Opin. Ther. Pat.* **1999**, *9*, 129−33.
(13) Woska, J. R., Jr.; Shih, D.; Kelly, T. A.; Taqueti, V. R.; Hogg, N.; Kishimoto, T. K. *J. Leukocyte Biol.*, in press.
(14) Springer, T. A. *Proc. Natl. Acad. Sci. U.S.A.* **1997**, *94*, 65−72.
(15) For a schematic diagram of integrin structure and function, see: Leitinger, B.; Hogg, N. *Nat. Struct. Biol.* **2000**, *7*, 614.
(16) Bella, J.; Kolatkar, P. R.; Marlor, C. W.; Greves, J. M.; Rossmann, M. G. *Proc. Natl. Acad. Sci. U.S.A.* **1998**, *95*, 4140−5.
(17) Ockenhouse, C. F.; Betageri, R.; Springer, T. A.; Staunton, D. E. *Cell* **1992**, *68*, 63−9.
(18) Berendt, A. R.; McDowall, A.; Craig, A. G.; Bates, P. A.; Sternberg, M. J.; Marsh, K.; Newbold, C. I.; Hogg, N. *Cell* **1992**, *68*, 71−81.
(19) Stanley, P.; Bates, P. A.; Harvey, J.; Bennett, R. I.; Hogg, N. *EMBO J.* **1994**, *13*, 1790−8.
(20) Randi, A. M.; Hogg, N. *J. Biol. Chem.* **1994**, *269*, 12395−8.
(21) Kamata, T.; Wright, R.; Takada, Y. *J. Biol. Chem.* **1995**, *270*, 12531−5.
(22) Edwards, C. P.; Champe, M.; Gonzalez, T.; Wessinger, M. E.; Spencer, S. A.; Presta, L. G.; Berman, P. W.; Bodary, S. C. *J. Biol. Chem.* **1995**, *270*, 12635−40.
(23) Huang, C.; Springer, T. A. *J. Biol. Chem.* **1995**, *270*, 19008−16.
(24) Edwards, C. P.; Fischer, K. L.; Presta, L. G.; Bodary, S. C. *J. Biol. Chem.* **1998**, *273*, 28937−44.
(25) Michishita, M.; Viden, V.; Arnout, M. A. *Cell* **1993**, *72*, 857−67.
(26) Stanley, P.; Hogg, N. *J. Biol. Chem.* **1998**, *273*, 3358−62.
(27) Ojima, I.; Bounaud, P.-Y.; Takeuchi, C.; Pera, P.; Bernacki, R. J. *Bioorg. Med. Chem. Lett.* **1998**, *8*, 189−94.
(28) Prestwich, G. D.; Dorman, G.; Elliott, J. T.; Marecak, D. M.;. Chaudhary, A. *Photochem. Photobiol.* **1997**, *65*, 222−34.

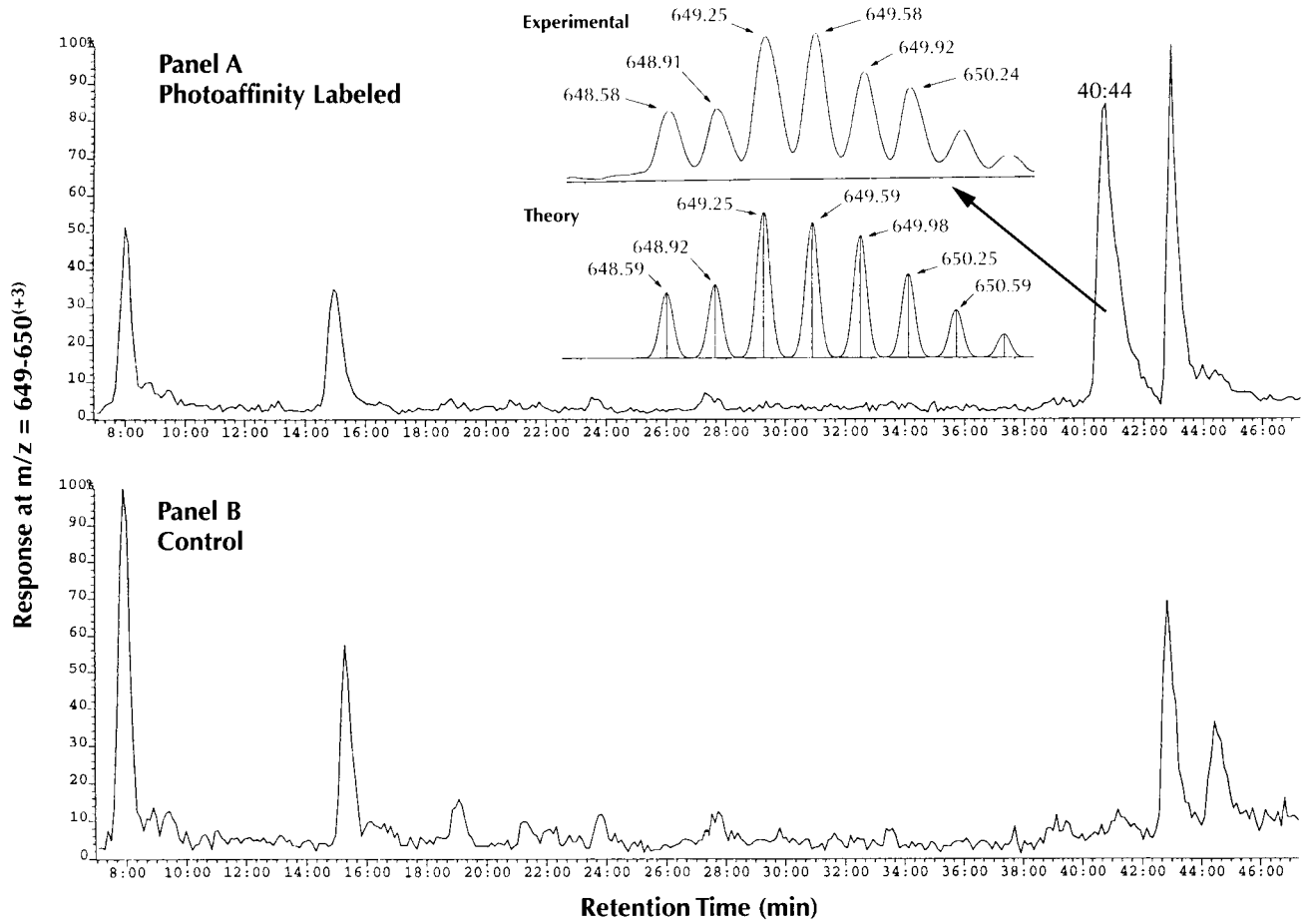

Figure 1. LC/MS of the trypsin digest of rCD11a I-domain photoaffinity labeled with **2**. The extracted mass chromatograms for $m/z = 649-650$ ($^{+}2$ charge state for mass 1945) for photoaffinity-labeled and control samples are shown in panels A and B, respectively. The peak eluting at 40 min 44 s is not present in the control. The inset in the upper panel shows the partial mass spectrum obtained for this peak (top) and the theoretical isotopic distribution calculated for the $^{+}3$ ion formed from residues 277−287 with label (bottom).

ESI MS technique, and the map was screened for the theoretical masses calculated above. These were plotted and compared to the map of the unlabeled sample.

Mass chromatograms for $m/z = 649-650$ ($^{+}3$ charge state for a component of monoisotopic mass 1945, Figure 1) revealed a component consistent with a photolabeled peptide containing the amino acid sequence FASKPASEFVK corresponding to amino acid residues 277−287 of the I-domain. The $^{+}2$ charge state ($m/z = 973-975$) for this component was also observed. The presence of one bromine and two chlorine atoms in the photoprobe produced a distinct isotopic distribution pattern unlike that produced by unlabeled peptides, confirming the identity of the specifically labeled tryptic fragment (Figure 1, upper chromatogram, inset).

Identification of the specific amino acid residue labeled by the benzophenone photoprobe was determined by LC/MS/MS analysis of the tryptic digest as shown in Figure 2. The daughter ion spectra from both the C-terminal and from the N-terminal fragments conclusively assigned the site of photolabel attachment to proline 281.

Several structural analogues of BIRT377 were shown to reduce the level of photoaffinity labeling of the I-domain by **2**. A positive correlation was observed between potency in the LFA-1/ICAM-1 binding assay and the level of protection from photoaffinity labeling (data not shown), indicating that the photoaffinity probe **2** is binding to the I-domain in a functionally relevant manner.

Knowledge of the exact site of benzophenone attachment provided a means for focused modeling experiments aimed at docking the antagonists into the published coordinates of the X-ray crystal structure of the I-domain.[29] These calculations were performed using a combination of automated docking procedures,[30,31] molecular dynamics simulations (MD),[32] and energy minimization.[32] For simplification of analysis, a larger hydantoin analogue (**3**; Chart 1) was used for the modeling experiments.

The docking was confined to a 30-Å cubic area with the center defined in the proximity of proline 281. Monte Carlo-simulated annealing conformational flexible docking of **3** was performed using a noncovalent van der Waals and electrostatic grid-based method of energy evaluation (0.5-Å resolution).[30,31] A rank ordering of the docking models was generated based on both agreement with observed structure−activity relationship (SAR) studies for the series and a suitable orientation of the hydantoin $N-CH_3$ bond vector toward the labeled proline 281 residue. Upon applying these criteria, a single viable docking model remained and was used as the starting geometry for refinement. A molecular dynamics (MD) simulation was carried

(29) Qu, A.; Leahy, D. J. *Proc. Natl. Acad. Sci. U.S.A.* **1995**, *92*, 10277−81.

(30) Morris, G. M.; Goodsell, D. S.; Huey, R.; Olson, A. J. *J. Computer-Aided Mol. Des.* **1996**, *10*, 293−304.

(31) Goodsell, D. S.; Olson, A. J. *Proteins* **1990**, *8*, 195−202.

(32) Brooks, B. R.; Bruccoleri, R. E.; Olafson, B. D.; States, D. J.; Swaminathan, S.; Karplus, M. . *J. Comput. Chem.* **1983**, *4*, 187−217.

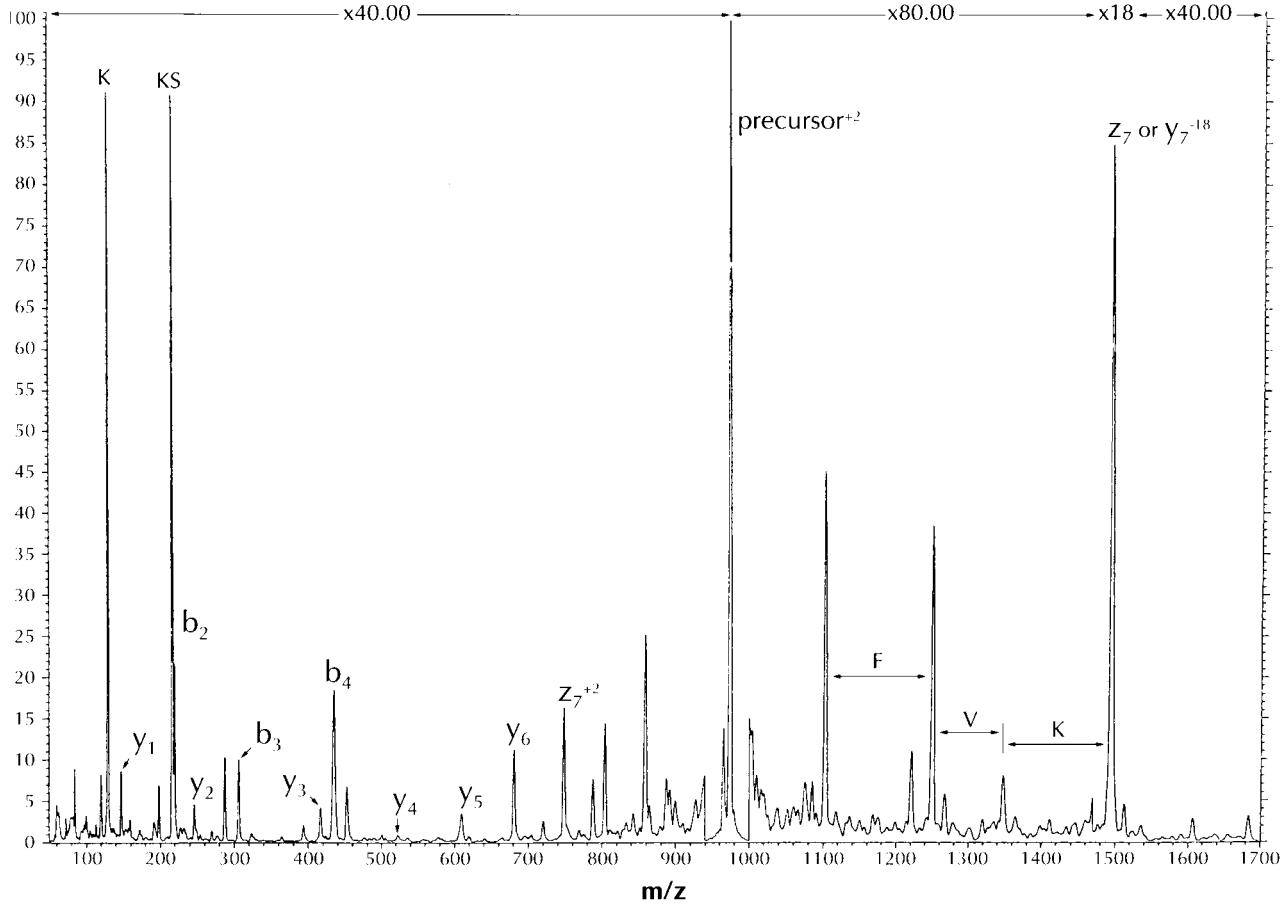

Figure 2. Daughter ion spectrum of photolabeled peptide. The MS/MS spectrum obtained from the $^{+}2$ ion isotope at $m/z = 973.9$ corresponding to photolabeled residues 277−287. The first seven C-terminal ions (y and z)[43] are observed with the added mass of label only at the seventh residue from the C-terminus. The first four N-terminal residues ions (b) are also observed without the added mass of label. Internal fragmentations were also observed, as indicated. The data conclusively support assignment of the site of photolabeling at Pro 281.

out on the protein/ligand complex with explicit water to account for solvation.[32] The MD average and 10 structures regularly spaced along the trajectory path were chosen for final energy minimization.

Analysis of the minimized structures showed a single common geometry for the complex between **3** and the LFA-1 I-domain. Figure 3a shows this final orientation of the antagonist at the proposed binding site. The carbon atom of the *N*-methyl group of **3** is ~9.4 Å away from the closest carbon atom of the labeled proline 281. This distance is consistent with the length of the reactive photoaffinity moiety of **2**.

Compound **3** is located on the protein surface opposite to the ICAM binding (MIDAS) site. The binding site is mainly hydrophobic in nature with some solvent exposure. The dichlorophenyl substituent binds in a well-defined hydrophobic pocket (Figure 4a). This pocket is formed exclusively by hydrophobic residues from β-strands 1, 3, and 4 and α-helices 1 and 7. The biphenyl moiety binds to another hydrophobic area (Figure 4b), closer to the protein surface with the distal phenyl group inserted between α-helices 1 and 7. The central hydantoin ring has some solvent-exposed areas and it does not make any specific electrostatic or H-bond interactions with the protein. It is likely, however, that this ring may contribute to stabilization of the bound conformation by orienting the two aromatic rings in a favorable edge-to-face aromatic/aromatic interaction.

The structure of the binding site is consistent with SAR studies (manuscript in preparation) that indicate that the compounds bind to LFA-1 solely through the use of nonionic interactions. Furthermore, the relative sizes of the two lipophilic pockets predicted from these studies, as well as the proposed binding conformation in which the aromatic rings of BIRT377 are in an edge-to-face orientation, have been confirmed.

After completion of the binding site identification studies, the X-ray crystal structure of the complex between LFA-1 I-domain and **4** (Chart 1) was obtained in our laboratories. The crystal structure confirmed the postulated binding mode for this series of hydantoin derivatives. Figure 3b shows a superposition of the X-ray crystal structure and the model structure for the complex; the rms deviation for the ligand is 0.63 Å, demonstrating the high quality of the predicted model. The details of this structure will be published in due course.

The identification of the binding site of the hydantoin antagonists provides important insight into the mechanism by which these molecules inhibit LFA-1 function. The location of the binding site, when coupled with several other lines of investigation, supports the hypothesis that the compounds prevent an allosteric change required for LFA-1 to access a conformation that binds ICAM-1. The alternative hypothesis that the compounds act by competing with ligand at the protein/protein interface is inconsistent with the current data which demonstrate that the antagonists bind at a location distal from the metal ion-binding site known to interact directly with a glutamate residue on ICAM-1 (Figure 3a).[19−25]

Integrins are known to undergo conformational regulation of activity that can be monitored by antibodies that detect epitopes

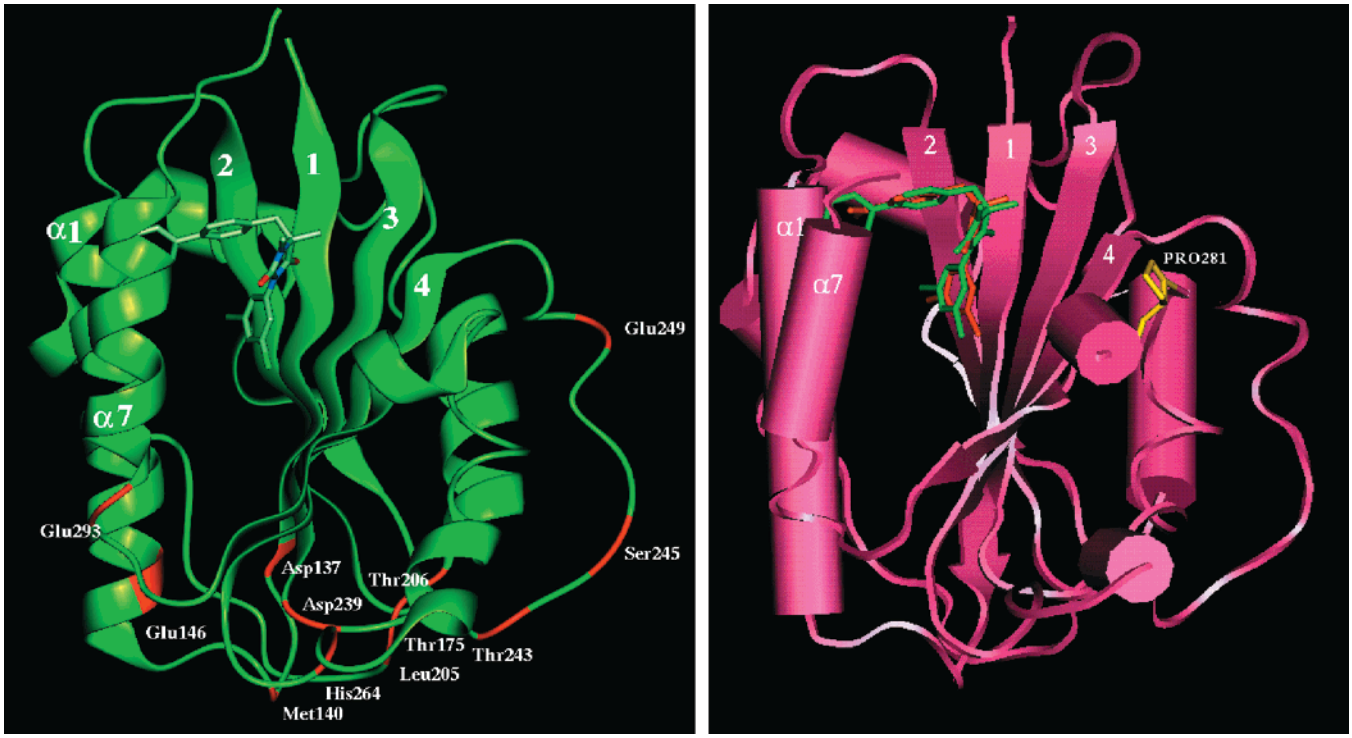

Figure 3. Structure of Cd11a I-domain/hydantoin complex. (a, left panel) Ribbon representation of computational model of **3** bound to LFA-1 I-domain. The highlighted residues (red) correspond to amino acids known to be critical for ICAM binding.[17−26] The inhibitor **3** is shown in stick representation. The biphenyl group is oriented toward α helices 1 and 7. The dichloro phenyl is between α helices 1, 7 and *β* strands 2, 1, and 3. (b, right panel) Comparison of computational and crystallographic models of LFA-I-domain (magenta). The binding mode orientation of **3** obtained from docking and MD simulation is shown in green. The binding mode observed in the X-ray crystal structure of **4** is shown in orange. Proline 281 is highlighted in yellow.

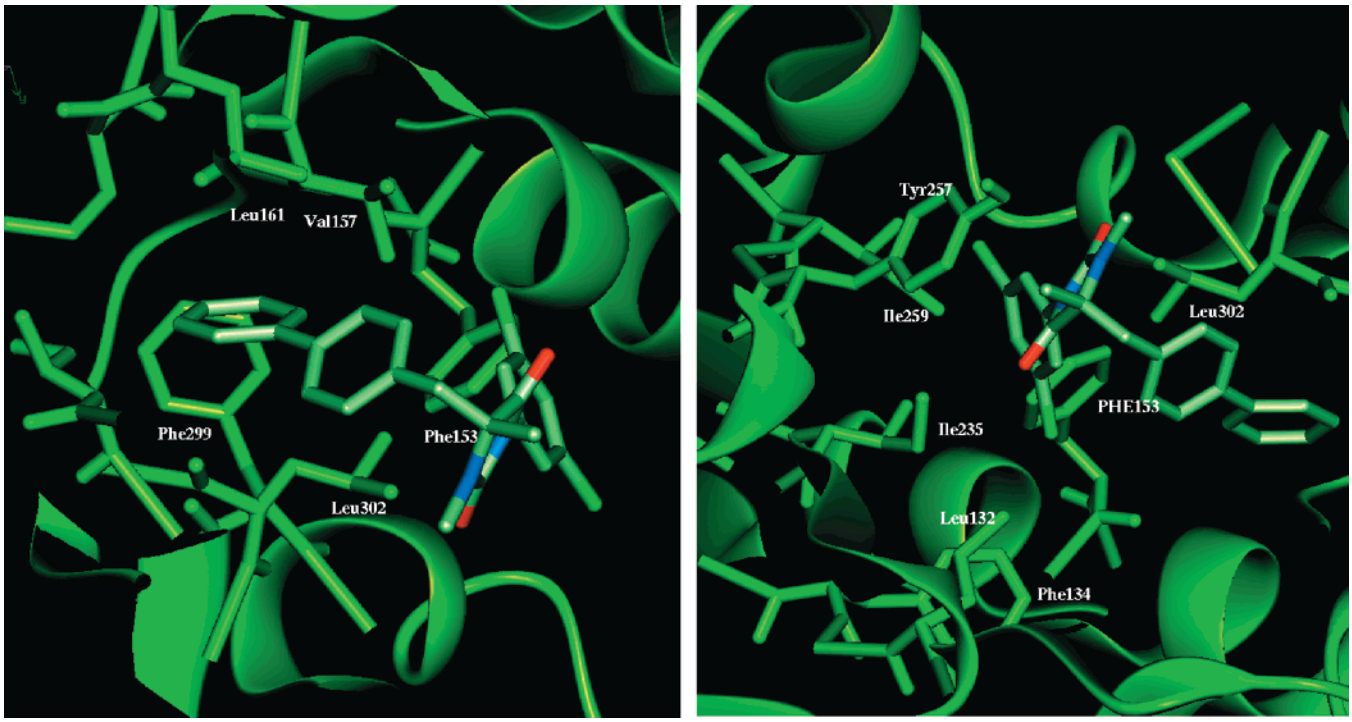

Figure 4. Binding site characteristics of **3** docked to LFA-1 I-domain. (a, left panel). Hydrophobic pocket for biphenyl moiety. Amino acid residues in contact with inhibitor are from α helices 1 and 7. (b, right panel) Hydrophobic pocket for dichlorophenyl moiety. Residues in contact with inhibitor are from α helices 1 and 7 and *β* strands 2, 1, and 3.

expressed only on high-affinity conformations.[33,34] In particular, activated SKW3 cells present the mAb24 epitope that is associated with ICAM-1 binding.[35] In addition to preventing ICAM-1 from binding to these cells, the binding of mAb24 is

(33) Frelinger, A. L., III; Cohen, I.; Plow, E. F.; Smith, M. A.; Robert, J.; Lam S. C−T.; Ginsberg, M. H. *J. Biol. Chem.* **1990**, *265*, 6346−52.

(34) Mould, A. P.; Garratt, A. N.; Askari, J. A.; Akiyama, S. K.; Humphries, M. J. *FEBS Lett.* **1995**, *363*, 118−22.

also blocked by BIRT377,[13] indicating that the high-affinity conformation of LFA-1 cannot be accessed in the presence of the compound.

The conformational changes associated with activation are consistent with a proposed model for the structure of integrin α subunits.[14,15] The model depicts the integrin α chain as a β-propeller fold with the I-domain linked via a "hinge" to the upper surface of this motif. Crystal structures demonstrate that the N- and the C-termini of the I-domain are in close proximity to each other and would form important components of the connection to the β-propeller.[29] If the relative position of the I-domain and β-propeller is important for ligand (e.g., ICAM) recognition, it seems reasonable that a small-molecule inhibitor bound near this "hinge" region would bias the positioning of the two domains and disrupt ligand binding.

The hydantoins in the current study bind at and form close contacts with the C-terminal α7 helix. This helix has shown a propensity for rigid body motion in NMR[36] and crystal structures[37] suggesting that it could be associated with changes in the overall conformation of the whole protein. While this motion could be an artifact of the use of a truncated protein,[38] it is consistent with recent X-ray crystal structures of the related collagen receptor (integrin $\alpha_2\beta_1$) I-domain in the presence and absence of bound ligand.[39] These structures show dramatic differences in the position of the C-terminal α6 and α7 helices between the conformations representing liganded and unliganded α_2 I-domain. The relative position of the α6 and α7 helices in the structure of the LFA-1 I-domain bound with the hydantoin antagonist corresponds closely to that seen in the unliganded (i.e., nonbinding) form of the collagen receptor (see ref 15 for a visual model).

Recently, other reports pointing to the critical regulatory role of the C-terminal helices of the β_2 integrin I-domains have appeared. Huth et al. have demonstrated that ICAM binding perturbs the NMR spectrum of the LFA-1 I-domain both at the MIDAS region and at the C-terminal portion of the protein.[40] They have also demonstrated that mutations in the I-domain near the C-terminal α-helix can result in constitutively active LFA-1. Recently, Shimaoka et al. used computational methods to design mutant Mac-1 I-domains that are stabilized in either the crystallographically defined C-terminal open or closed conformations.[41] The open (but not the closed) form of the I-domains successfully bind the ligand iC3b. These results demonstrate that the positioning of the C-terminal helices is coupled to the ligand-binding capacity of the MIDAS region in the β_2 integrins.

There have also been reports that other small molecules bind to the C-terminus of the LFA-1 I-domain. In particular, the structure of lovastatin bound to the LFA-1 I-domain has been disclosed.[42] The ability of two structurally distinct molecules to target a regulatory site encourages the belief that a general strategy for designing inhibitors of protein conformational changes could be based on this approach.

The location of the binding site, the potent functional inhibition of ICAM-1 binding, and the blocking of activation epitopes on LFA-1 all indicate that the hydantoins are binding to LFA-1 and sequestering it in a conformation that is unable to interact with ICAM-1. This allosteric regulation of integrin function presents an alternate means of blocking protein/protein interactions from the traditional approach of epitope mimicry wherein critical surface contacts are identified via mutagenesis and small molecules are designed around these amino acid residues.

Disruption of the LFA-1/ICAM interaction is currently undergoing clinical testing with biological reagents directed against these proteins and may allow for therapeutic intervention in inflammatory and immunological diseases. The small molecules discussed herein represent an advance in this arena in that antagonism of this event can now be achieved with orally bioavailable heterocyclic molecules. In this report, we have described the specific binding site of these molecules on LFA-1. The information from the binding site studies has also contributed to the understanding of regulation of protein conformation at the atomic level.

Experimental Section

Synthesis of Photoprobe 2. Phthalimide (6). To a solution of hydantoin **5**[44] (0.50 g, 1.17 mmol) in dry DMF (5.0 mL) at 0 °C under argon was added potassium bis(trimethylsilyl)amide (2.6 mL, 1.30 mmol). The resultant mixture was stirred for 5 min at 0 °C. A solution of *N*-(4-bromobutyl)phthalimide (0.66 g, 2.34 mmol) in dry DMF (5.0 mL) was then added dropwise. The solution was stirred at 0 °C for 30 min followed by removal of the ice bath and stirring at room temperature for 30 min. The solution was poured into aqueous 1 N HCl solution and extracted with ethyl acetate. The combined organic phases were washed once sequentially with aqueous 1 N HCl solution, aqueous saturated $NaHCO_3$ solution, water, and aqueous saturated NaCl solution. The organic layer was concentrated in vacuo. The residue was purified by flash chromatography (SiO_2, 9:1−1:1 hexanes/ethyl acetate) to give phthalimide **6**, 588.7 mg (80%) which contained some remaining **5**: ^{1}H NMR (400 MHz, $CDCl_3$) δ 7.79 (dd, J = 3.1, 5.4 Hz, 2H), 7.67 (dd, J = 3.1, 5.4 Hz, 2H), 7.36 (d, J = 8.3 Hz, 2H), 7.21 (t, J = 1.6 Hz, 1H), 6.90 (d, J = 8.3 Hz, 2H), 6.82 (d, J = 1.6 Hz, 2H), 8.82−3.70 (m, 3H), 3.33−3.23 (m, 1H), 3.04 (d, J = 14.1 Hz, 1H), 2.99 (d, J = 14.1 Hz, 1H), 1.95−1.62 (m, 7H).

Amine Hydrochloride (7). To a solution of phthalimide **6** (20.0 mg, 0.032 mmol) in absolute ethanol (2.0 mL) was added a solution of methylamine in ethanol (0.53 mL, 8.03 M in ethanol, 4.26 mmol). The mixture was heated to reflux under argon for 2.5 h. The solution was allowed to cool to room temperature and concentrated in vacuo. The residue was partitioned between water and dichloromethane. The aqueous layer was extracted with dichloromethane. The combined organic layers were washed with aqueous saturated NaCl solution and concentrated in vacuo. The residue was dissolved in absolute ethanol, and hydrogen chloride was bubbled through the solution for 30 min. The mixture was sealed and allowed to stand for 11 h. The solvent was removed in vacuo, and the remaining material was triturated with anhydrous ether. The solid was dried in vacuo to give 32.1 mg (54%) of amine hydrochloride **7**: ^{1}H NMR (400 MHz, $CDCl_3$) δ 7.58 (t, J = 1.3 Hz, 1H), 7.50 (d, J = 8.2 Hz, 2H), 7.02 (d, J = 8.2 Hz, 2H), 6.90 (d, J = 1.3 Hz, 2H), 4.2−4.0 (br s, 1H), 3.6−3.3 (m, 2H), 3.30 (d, J = 13.2 Hz, 1H), 3.19 (d, J = 13.2 Hz, 1H), 2.9−2.7 (br s, 2H), 1.8−1.5 (m, 5H); MS (CI) 498 (MH^+); HPLC (C-18 reversed-phase Rainin

(35) Dransfield, I.; Hogg, N. *EMBO J.* **1989**, *8*, 3759−65.
(36) Legge, G. B.; Kriwacki, R. W.; Chung, J.; Hommel, U.; Ramage, P.; Case, D. A.; Dyson. H. J.; Wright, P. E. *J. Mol. Biol.* **2000**, *295*, 1251−64.
(37) Lee, J. O.; Arnaout, M. A.; Liddington, R. C. *Structure* **1995**, *3*, 1333−40.
(38) Baldwin, E. T.; Sarver, R. W.; Bryantm, G. L., Jr.; Gurry, K. A.; Fairbanks, M. B.; Finzel, B. C.; Garlick, R. L.; Heinrikson, R. L.; Horton, N. C.; Kelley, L. L.; Mildner, A. L.; Moon, J. B.; Mott, J. E.; Mutchler, V. T.; Tomich, C. S.; Watenpaugh, K. D.; Wiley: V. H. *Structure* **1998**, *6*, 923−35.
(39) Emsley, J.; Knight, C. G.; Farndale, R. W.; Barnes, M. J.; Liddington, R. C. *Cell* **2000**, *101*, 47−56.
(40) Huth, J. R.; Olejniczak, E. T.; Mendoza, R.; Liang, H.; Harris, E. A. S.; Lupher, M. L., Jr.; Wilson, A. E.; Fesik, S. W.; Staunton, D. E. *Proc. Natl. Acad. Sci. U.S.A.* **2000**, *97*, 5231−6.
(41) Shimaoka, M.; Shifman, J. M.; Jing, H.; Takagi, J.; Mayo, S. L.; Springer, T. A. *Nat. Struct. Biol.* **2000**, *7*, 674−8.
(42) Kallen, J.; Welzenbach, K.; Ramage, P.; Geyl, D.; Kriwacki, R.; Legge, G.; Cottens, S.; Weitz-Schmidt, G.; Hommel, U. *J. Mol. Biol.* **1999**, *292*, 1−9.
(43) Biemann, K. *Biomed. Environ. Mass Spectrom.* **1988**, *16*, 99−111.
(44) Yee, N. K. *Org. Lett.* **2000**, *2*, 2781−3.

Microsorb 80−220-C5, 5 μm, 21.4 mm × 25 cm, isocratic 90% methanol in water over 21 min, 10 mL/min) retention time 5.1 min, purity 97.5% (UV, λ = 254 nm).

Photoprobe 2. To a DMF (0.50 mL) solution of amine hydrochloride **7** (12.5 mg, 0.025 mmol), 3-(4-benzoylphenyl)propanoic acid (6.7 mg, 0.026 mmol), and 1-hydroxybenzotriazole (3.7 mg, 0.027 mmol) at room temperature under argon was added diisopropylethylamine (30.4 L, 0.174 mmol). The solution was stirred for 30 min. EDC (5.1 mg, 0.027 mmol) was added as a solid in one portion, and the resultant solution was stirred at room temperature under argon overnight. The solution was poured into 1 N aqueous HCl solution and extracted with ethyl acetate. The combined organic layers were washed once with 1 N HCl solution, twice with aqueous saturated $NaHCO_3$ solution, and once with aqueous saturated NaCl solution. The organic layer was dried with anhydrous Na_2SO_4, filtered, and concentrated in vacuo. The crude product was purified by preparative TLC (SiO_2, 1000 $\mu\mu$, 20 × 20 cm, ethyl acetate) to give 14.2 mg (77%) of photoprobe **2**: ^{1}H NMR (400 MHz, $CDCl_3$) δ 7.80 (d, J = 7.2 Hz, 2H), 7.75 (d, J = 8.1 Hz, 2H), 7.61 (t, J = 7.4 Hz, 1H), 7.53−7.45 (m, 2H), 7.42 (d, J = 8.24 Hz, 2H), 7.33 (d, J = 8.1 H, 2H), 7.30 (t, J = 1.7 Hz, 1H), 6.94 (d, J = 8.3 Hz, 2H), 8.85 (d, J = 1.7 Hz, 2H), 5.71 (t, J = 5.6 Hz, 1H), 3.73−3.64 (m, 1H), 3.42−2.97 (m, 7H), 2.53 (t, J = 7.6 Hz, 2H), 1.83−1.47 (m, 7H); electrospray MS 735.9 (MH^+), 757.9 ($M + Na^+$); HPLC (C-18 reversed-phase Zorbax SB-C18 column, 5 μm, 4.6 × 150 mm, linear gradient 50−100% acetonitrile in water over 35 min, 0.5 mL/min) retention time 25.21 min, purity (UV, λ = 254 nm) 100%.

Purification of Recombinant LFA-1 I-Domain Protein. Several constructs of the CD11a I-domain recombinantly expressed in *Escherichia coli* were used in these studies. GST-I-domain constructs (KLB4.3, Cys^{125}−Gly^{311}; KLB5.3, Cys^{125}−Ser^{325} + C-term tag; THpCR2.10, Leu^{111}−Ser^{327}) were generated using the pGEX2T (Pharmacia) vector adapting the methods used by Michishita.[25] A fourth CD11a I-domain construct was generated using the pET11a (Stratagene) vector (KLB14.2.1, Cys^{125}−Gly^{311}). This construct was purified and refolded by adaption of the methods of Qu and Leahy.[29] All constructs were made by PCR from full-length LFA-1α cDNA. The oligonucleotides used for each construct added restriction sites to the 5′and 3′ ends. Restriction digested products were then ligated into their vectors. The predicted sizes of the proteins (~50 kDa for the GST-fusion proteins, ~24 kDa for the thrombin-cleaved proteins, and ~21 kDa for the refolded form) corresponded to the electrophoretic mobility of the isolated proteins as determined by SDS−PAGE. All constructs expressed at least six mAb epitopes, four of which had been identified as I-domain epitopes (data not shown).

Inhibition of Ab Binding to I-Domain by BIRT 377. mAb R3.1 was generated in-house, and biotinylated mAb38 was obtained from Southern Biotech. ELISA assays were performed in standard 96-well format with the following modifications. All steps were carried out at 37 °C. Gelatin (2%, Bio-Rad) in D-PBS (Gibco/BRL) was used as the blocking agent and was reduced to 0.5% as diluent throughout the assay. Washes were done in D-PBS supplemented with 1 mM $MgCl_2$. Plates (NalgeNUNC) were coated with 20 μg/mL mAB R3.1, incubated, washed, and blocked. Compound and I-domain (KLB4.3) were added simultaneously to the plate. Following an incubation and wash, biotinylated mAB38 was added and binding was assessed by SA-HRP (Zymed). The addition of ABTS (Zymed) resulted in color development. Signal was read at 405 nm on a microplate reader (Molecular Devices). BIRT 377 showed full dose-responsive behavior in this assay with an approximate IC_{50} = 0.5 μM.

Photoaffinity Labeling Experiments. The rCD11a I-domain (construct KLB5.3, 10 mM TRIS, pH 8, 5 mM β-mercaptoethanol, 5 mM $MgCl_2$) was incubated for 60 min in the dark with a 5-fold molar excess of **2** (or DMSO control) and then photolyzed for 45 min. at 4 °C with 3000 μW/cm^2 light intensity (maximum output at 350 nm). The I-domain was denatured by the addition of an equal volume of 8 M urea in 0.4 M ammonium bicarbonate, reduced with DTT at 50 °C, carboxamido-methylated with iodoacetamide at 50 °C, and digested to completion with trypsin for 20 h at 37 °C. The digests were stored at −80 °C prior to LC/MS analysis.

Mass Spectrometry. Identification of the labeled tryptic peptide was performed on an Autospec mass spectrometer (Micromass, Manchester, U.K.). A magnet scan from m/z = 1800 to 400 at 8 s/decade was employed to obtain survey data for detection of photoaffinity-labeled peptides. A voltage scan from m/z = 977−970 at 4 s/scan was employed to enhance the signal-to-noise ratio and accuracy in verifying the labeled peptide. Data were acquired in profile mode, at 2500 resolution. The LC conditions were as follows: 150 × 0.30 mm C18 300-Å column (LC Packings), 10-μL injection, mobile phase A 95:5:0.6 water/acetonitrile/TFA, mobile B 95:5:0.52 acetonitrile/water/TFA, programmed from 0 to 100% B in a complex gradient over 70 min. The magnet survey scan data were analyzed exhaustively. The mass of the photolabel was added to each predicted tryptic peptide including peptides formed via missed cleavages. This was used to generate a list of m/z values for the charge states of each potential labeled peptide. The HPLC trace of the photolabeled tryptic digest was plotted for each theoretical m/z. Positive results were compared to the control digest. Responses not present in the control were further analyzed for the presence of confirmatory coelution of related charge states or confirmation of charge state via isotopic spacing. The LC/MS/MS experiments were performed on an Autospec OATOF (Micromass). The precursor ion was selected at 1200 resolution at 973.9 (MH_2^{2+}). The collision gas was methane (50% reduction of parent ion intensity), 200 eV collision energy. Daughter ion (TOF) spectra were acquired in profile mode at 8 s/spectrum and averaged over the HPLC peak. The LC conditions were as follows: 150 × 0.30 mm Pepmap C18 column (LC Packings, San Francisco, CA) 20-μL injection, flow 3 μL/min. Mobile phase was 99:1:0.1 water/acetonitrile/formic acid, and mobile B was 90:10:0.1 acetonitrile/water/formic acid programmed from 0 to 100% B in a complex gradient over 75 min.

The LC/MS experiments for assessment of competition of photolabeling were performed on an API III 3+ mass spectrometer (PE Sciex, Toronto, Canada). The triply and doubly charged molecular ions for the labeled peptide and doubly charged molecular ion for the corresponding unlabeled peptide were monitored at m/z = 605, 649, and 973, with a 5 amu window using a 75-ms dwell and 0.2 amu step. A 70-V orifice voltage was employed. The LC conditions were as follows: 150 × 1 mm Jupiter C18 300 Å (Phenomenex, Torrance CA) 40 μL/min flow, 10-μL injection. A and B mobile phases as noted above, programmed from 0 to 10% B at 10 min to 60% B at 40 min to 100% B at 55 min.

Competition Experiments. Competition experiments were done by incubating the rCD11a I-domain (constructs KLB14.2.1 or THpCR2.10) with a 6−10-fold molar excess (vs protein) of competitor (or DMSO) for 30 min. A 5-fold molar excess of **2** (vs protein) was then added to each sample. Photolabeling and irradiation followed by tryptic digestion were then carried out as noted above. Protection was calculated as a reduction in percentage response of the labeled peptide (relative to unlabeled peptide) by monitoring the $^+2$ charge state of the unlabeled peptide at m/z = 605 and the $^+2$ charge state of the labeled peptide at m/z = 973.

Molecular Modeling. The docking experiments were performed using the Autodock package v. 2.0[30,31] using coordinates from a previously published X-ray crystal structure of LFA-1 I-domain.[29] The steric grid representing the protein was computed using the default Autodock force field; 6−12 Lennard-Jones parameters for chlorine were added using the standard Amber force field.[45] The electrostatic Autodock grid was computed using charmM extended atom force field charges. The grid was defined as a 30 × 30 × 30 Å box centered in the proximity of proline 281. The inhibitor geometry was optimized with an ab initio method using a 6-31G* basis set.[46] The ESP charges were then computed using the CHELPG option in Gaussian94.[47] Fifty

(45) Weiner, S. J.; Kollman, P. A.; Case, D. A.; Singh, U. C.; Ghio, C.; Alagona, G.; Profeta, S., Jr.; Weiner, P. *J. Am. Chem. Soc.* **1984**, *106*, 765−84.

(46) Gaussian 94 (Revision 94_D2), Frisch, M. J.; Trucks, G. W.; Schlegel, H. B.; Gill, P. M. W.; Johnson, B. G.; Robb, M. A.; Cheeseman, J. R.; Keith, T. A.; Petersson, G. A.; Montgomery, J. A.; Raghavachari, K.; Al-Laham, M. A.; Zakrewski, V. G.; Ortiz, J. V.; Foresman, J. B.; Cioslowski, J.; Stefanov, B. B.; Nanayakkara, A.; Challacombe, M.; Peng, C. Y.; Ayala, P. Y.; Chen, W.; Wong, M. W.; Andres, J. L.; Replogle, E. S.; Gomperts, R.; Martin, R. L.; Fox, D. J.; Brinkley, J. S.; Defrees, D. J.; Baker, J.; Stewart, J. P.; Head-Gordon, M.; Gonzalez, C.; Pople, J. A. Gaussian, Inc., Pittsburgh, PA, 1995.

Autodock runs of 100 000 Monte Carlo steps were performed and the top 50 orientations were selected for further analysis. Molecular dynamics simulations of the protein/inhibitor complex were performed using the CHARMm program from Molecular Simulations Inc.[30] The all-atoms force field was used with explicit TIP3P water molecule model.[48] Solvent effect was represented using a 25-Å water sphere (cup model). The center of the sphere was located at C-5 of the hydantoin ring. All the atoms within 13 Å of the inhibitor were allowed to move during the simulation. The rest of the atoms in the protein were tethered using a force constant of 1 kcal mol^{-1} $Å^{-3}$. The water molecules located further than 13 Å were maintained within the water sphere using the DROP CHARMm command with default values. The nonbonding van der Waals interactions were computed using a switch cutoff function from 9 to 11 Å and a complete cutoff from 11 Å. The nonbonding electrostatic energy was computed using a dielectric constant of 1. A shift cutoff function from 9 to 11 Å and a complete cutoff from 11 Å were used. All MD simulations were carried out with charmM at 298 K using a time step of 0.001 ps. Heating of the system was done at a rate of 1° every 10 MD steps. Equilibration was performed over 30 000 MD steps (30 ps). MD production was carried out for 1 ns. Energy minimization was performed using charmM with the ABNR minimizer and convergence criterion of 0.001.

Acknowledgment. The authors gratefully acknowledge the following individuals for helpful comments and suggestions: Robert Rothlein, Joseph R. Woska, Jr., T. Kei Kishimoto, and Richard Ingraham. Additionally, we thank Charles Cywin and Tin Min Htut for kindly providing reagents. Jim Langridge of Micromass (Manchester, U.K.) supplied preliminary LC/MS data (not shown in this report) which was of assistance in designing further experiments.

JA0104249

(47) Besler, B. H.; Merz, K. M., Jr.; Kollman, P. A. *J. Comput. Chem.* **1990**, *11*, 431−9.

(48) Jorgenson, W. L.; Madura, J. D. *Mol. Phys.* **1985**, *56*, 1381−92.